Uranium contamination removal from water by an orchid (*Vanda tessellata)* based biosorbent

Pritee Pandey[1] · Madhurima Pandey[1] · Piyush Kant Pandey[2]

Abstract

The study reports biosorptive removal of uranium(VI) water contamination by a wild epiphytic orchid plant: *Vanda tessellata*. This orchid plant was chosen based on abundant availability and adsorption efficacy. In batch mode operation the maximum uranium(VI) adsorption capacity was found as 416 μg g^{-1} of dry biomass. The optimum pH for adsorption was neutral (7), and the equilibrium time was 15 min at 30 $\pm$ 5 °C temperature. The adsorbent properties were characterized by SEM, EDS, and FTIR techniques. The effects of various variables like pH, initial ion concentration, biosorbent dose, contact time, and temperature on the adsorption process were studied. The Langmuir isotherm showed better agreement ($R^2 = 0.987$) to describe the adsorption process, and the adsorption process followed pseudo-second-order kinetics. The thermodynamic study showed the endothermic, and spontaneous nature of adsorption in a feasible manner. The adsorbent can be used for developing a remedial method for uranium contamination in the water.

Keywords Uranium · Water contamination · Adsorption · *Vanda-tessellata* · Radioactive element

Introduction

Uranium is a naturally occurring radioactive element and is toxic both chemically and radiologically. The chemical toxicity of water-soluble uranium supersedes its radiological toxicity. Uranium can be present in soluble form in water, and the water-soluble uranium is considered hazardous to the living beings on ingestion. On being metabolized, the uranium(VI) can enter the bloodstream and can cause damage to different body parts, especially to the kidney [1, 2]. The safe limit of uranium in drinking water is 30 μg L^{-1} in terms of chemical toxicity [3] and 60 μg L^{-1} in terms of radiological toxicity [4]. Uranium is reported as ubiquitous in the environment [5]. High chemical toxicity and universal abundance of uranium in groundwater is a matter of concern as it is hazardous to the health of residents of a contaminated area.

The hazards of water-soluble uranium to human health have fueled the interest in developing methods for the removal of uranium from contaminated water in the recent decades. The solid-phase extraction method is considered a primary choice for extracting metals from water because of the ease of application and processing safety. Thus, several solid-phase extraction methods have been developed, but most of them have used synthetic chemicals or chemically treated biomaterials as adsorbate [6–13]. Use of various novel compounds [14], complexing agents [15], nanomaterials [16–20], silica [21], silica nanoparticles [22, 23], and nano-size particles of metal oxides [24] have been reported with varying degree of efficiency. Yet most of the reported methods are either uneconomic or suffer from a possible hazardous waste byproduct. It was also noted that most of the reported methods operate at been applied to uranium solutions of high concentration [25], which could not be well efficient for uranium contamination at a low level.

The maximum concentration of uranium in underground water was reported as 770.1 μg L^{-1} in India [26–30], 840 μg L^{-1} in Canada [31], 267.8 μg L^{-1} in Nigeria [32], 92.02 μg L^{-1} in Switzerland [33] and 800 μg L^{-1} in Finland [34]. The above levels encouraged us to develop a new method for

✉ Piyush Kant Pandey
  piyushkant.researchid29@gmail.com;
  drpiyush_pandey@yahoo.com

1   Department of Applied Chemistry, Bhilai Institute of Technology, Durg, Bhilai House, Durg, Chhattisgarh 491001, India

2   LCIT Group of Institutions, High Court Road, Bilaspur, Chhattisgarh 495001, India

removing uranium from underground water, which should be cost-effective and efficient at a low concentration of uranium, preferably at neutral pH. Hence, this paper presents a detailed and systematic study for uranium removal from uranium contaminated solution and natural underground water by dried biomass, derived from an orchid plant *Vanda tessellata.* The candidate plant was chosen after a preliminary study with various other locally available plants for their ability to adsorb the soluble uranium from water. The other studied plants showed least ability to remove the soluble uranium except the *Vanda tessellata.* The literature study also indicated the presence of carbonyl functional groups [35] in the *Vanda tessellata.* As the carbonyl functional groups are known to cause strong coordination bonding with uranium ions [36], hence we focused on the detailed study of the orchid derived biomass based uranium removal study. Previously also, the *Vanda tessellata* has already been reported by us, as an effective biosorbent for removing lead and arsenic from water [37, 38] with good efficiency.

Experimental

Apparatus

The *Vanda tessellata* derived biosorbent was characterized by SEM (ZEISS EVO Series Scanning Electron Microscopic Model EVO 18) and EDS (INCA 250 EDS, X-MAX 20 mm Detector). The infrared spectra were recorded with FTIR Spectrometer (Thermo Fisher Scientific, Nicolet Is10, Madison, USA, equipped with a DLaTGS temperature stabilized detector). Uranium concentration in solution was examined by LED Fluorimeter, LF-2a of make QUNATALASE.

Reagents

Uranium stock solution of 100 mg L^{-1} (ICP-MS-66 N-0.01X-1 Uranium) was used to prepare uranium solution of different concentrations. Analytical grade (AR) chemicals viz. nitric acid, sodium pyrophosphate, orthophosphoric acid and sodium hydroxide were used in the experiments.

Preparation of the biomass from *Vanda tessellata*

The orchid plant, named *Vanda tessellata* was selected for this study based on a preliminary elimination of other locally available plants. The candidate orchid plant was collected from the forest area of central east Chhattisgarh. This plant species is available in Chhattisgarh and distributed throughout south-east Asia [39]. The orchid plant was manually collected from the trees in the forest. It was then washed to remove dust and other foreign particles and dried in sunlight

for 30 days, followed by in hot air oven at 80 °C for six days. Dried biomass was then grounded in a blender and screened through 150-micron mesh. The sieved biomass powder was safely stored in a sterile environment till its further use.

Pre-leaching of biomass

Biomass powder ($\leq$ 150-micron) was pre-leached by 1:1 HNO_3 for 3 h and then filtered through Whatmann filter paper no. 42. Filtered biomass was then washed with double distilled water till washing was found neutral. The resulting neutralized biomass was dried in a hot air oven at 50ºC, overnight.

Adsorption experiment

Adsorption of uranium(VI) was carried out in batch experiments initially at pH 7. Procedurally, about 100 mL of 100 µg L^{-1} uranium solution was treated with 0.1 g of leached biomass of particle size $\leq$ 150 µm and stirred by a magnetic stirrer for 15 min in a beaker. The solution was separated from adsorbate by filtration with Whatmann filter paper (42). The concentration of uranium in the filtrate was determined by a LED Fluorimeter, which is the instrument considered as the most accurate and reliable instrument for the determination of uranium in aqueous solution, even at a very low concentration of 0.1 µg L^{-1} [40]. The amount of uranium adsorbed on the biosorbent was calculated as the difference between uranium concentration in the solution, before and after adsorption.

The following formulae calculated the percentage removal of uranium, solid-phase uranium concentration (Adsorption efficiency) as q_e (µg g^{-1}) and distribution coefficient as K (L g^{-1}):

$$\%\text{Removal} = \frac{\left(C_i - C_f\right)}{C_i} \times 100 \tag{1}$$

$$q_e = \frac{\left(C_i - C_f\right)}{M} \times V \tag{2}$$

$$K = \frac{\left(C_i - C_f\right)}{C_f} \times \frac{V}{M} \tag{3}$$

C_i and C_f are initial and final uranium(VI) ion concentration in solution (µg L^{-1}), respectively, M is the amount of adsorbent used (g), and V is the volume of solution (L) [41].

The batch experiments were carried out at different pH (1–13), different contact time (1–120 min), and different temperatures (283 K to 333 K) in 100 mL of 100 µg L^{-1} uranium(VI) solution with 0.1 g of the adsorbent.

Experiments were also carried out with different initial ion concentration (10–500 μg L^{-1}) in 100 mL volume.

Quality assurance and quality control

Standard uranium stock solution of 100 mg L^{-1} (ICP-MS-66 N-0.01X-1 Uranium) was used to conduct experiments and calibration of the instrument. Standard lab accessories viz. micropipettes, analytical balance, etc. were used for preparing uranium solutions of different concentrations. A standard addition method was adopted to overcome the matrix effect. The average of four readings was taken for each measurement. The results obtained within ± 10% standard deviation was accepted. Triplicate experiments were conducted for each measurement. Uranium concentration

analysis was carried out at a constant temperature and in a dust-free environment.

Characterization of biomass

FTIR analysis

FTIR spectra of biomass treated with control sample (Control biomass) and the biomass treated with uranium(VI) (Uranium(VI) exposed biomass) were examined to identify the functional group of the biomass responsible for uranium(VI) adsorption. FTIR spectra of control biomass and uranium(VI) exposed biomass are given in Fig. 1a, b. The spectra of control biomass indicates a decrease in intensity and slight shifting in the position of the band, which
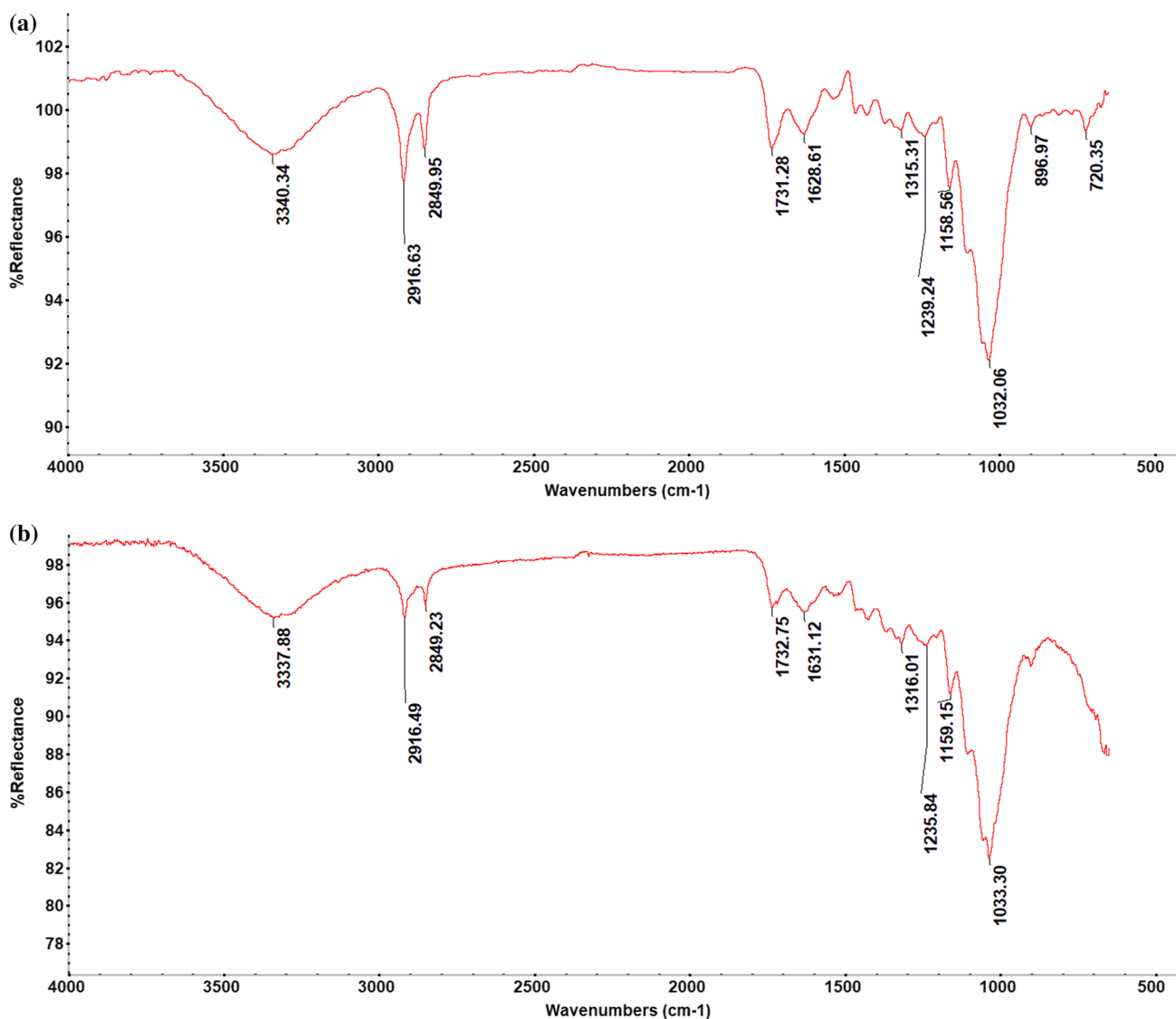

Fig. 1 FTIR of **a** control biomass **b** uranium(VI) exposed biomass

highlights the uranium(VI) abstraction without causing a change in the structure and composition of biomass.

Control biomass gave a strong and sharp peak at 3340 cm^{-1} due to N–H asymmetric stretching vibration of the protein group is broadened and shifted to 3337 cm^{-1} in uranium(VI) exposed biomass. The band at 1628 cm^{-1} in control biomass highlights the presence of N–H in-plane bending (amide II band) vibrations due to primary amide group was found to be shifted to 1631 cm^{-1} in uranium(VI) exposed loaded biomass.

A weak absorption band at 1239 cm^{-1} in control biomass was consistent with the asymmetrical C–O–C stretching vibration of the ether group. This band was found to be shifted to 1235 cm^{-1} in uranium(VI) exposed biomass. Further, a distinct peak was observed at 720 cm^{-1}, due to the OH out-of-plane band in the control sample. This peak disappeared in the uranium(VI) exposed sample, which explains the complexation of OH with uranium(VI) ions. FTIR study indicates the involvement of N–H, O–H, and C–O–C groups in the adsorption of uranium(VI) ions. Thus, the comparison between FTIR spectra of uranium(VI) exposed biomass and control biomass elucidate that nitrogen or oxygen atom coordinate with uranium(VI) ions [42, 43].

Scanning electron microscope (SEM) study

SEM is considered as most reliable method to study the changes in the surface or physical structure of solid substances. SEM images of biomass treated with control sample (Control Biomass) and the biomass treated with uranium(VI) (Uranium(VI) exposed biomass) are given in Fig. 2a, b. The micrograph of controlled biomass indicates the presence of a heterogeneous porous structure of the biomass surface. It is reported [44, 45] that ionic species

like UO$_2^{2+}$ are adsorbed by plant-based bio sorbents like rice stem due to the interaction of UO$_2^{2+}$ with the functional organic groups like the hydroxyl group, carbonyl group, silicon oxygen bond (Si–O), and phosphorous oxygen (P–O) etc.

Similarly, the probable ionic exchange of hydrogen ions with uranyl ions and diffusive filling of voids in biosorbent are attributed as the cause of filling of the voids thus disappearance of pores in the biomass [46].

In our experiment also a significant change in the morphology of uranium(VI) exposed biomass was observed which can be attributed to the possible reaction of the uranyl ions with the functional groups viz. N–H, O–H, and C–O–C groups (presence of such groups as established by FTIR analysis) and the filling of resultant products leading to the disappearance of surface voids.

Energy-dispersive X-ray spectroscopy (EDS) analysis

EDS study of biomass before and after adsorption of uranium(VI) *Vanda tessellata* biomass was carried out to confirm the incorporation of uranium(VI) ions on to the adsorbent. Energy-Dispersive X-ray spectra of the biomass before and after adsorption of uranium(VI) are given in Fig. 3a, b, and their percentage composition is given the Table 1. EDS of biomass before adsorption indicates the presence of C, O, Al, Ca, and Fe elements in the biomass. The EDS of the biomass after adsorption shows appearance of an additional peak of uranium. This appearance of a new peak, characterized as uranium, confirms the adsorption of uranium onto the biomass. Thus, the EDS study corroborates the results obtained by FTIR and SEM study results presented in the preceding paragraphs.

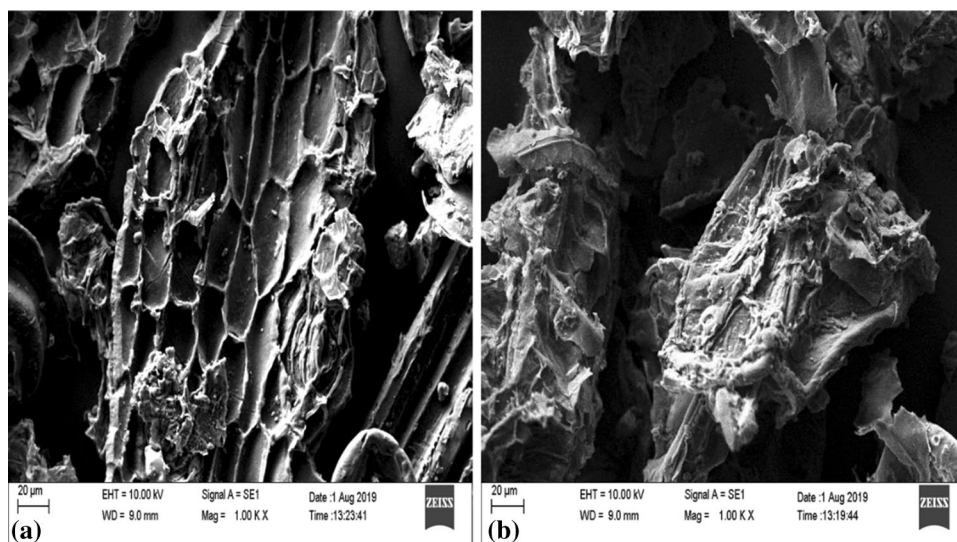**Fig. 2** SEM of **a** control biomass **b** uranium(VI) exposed biomass

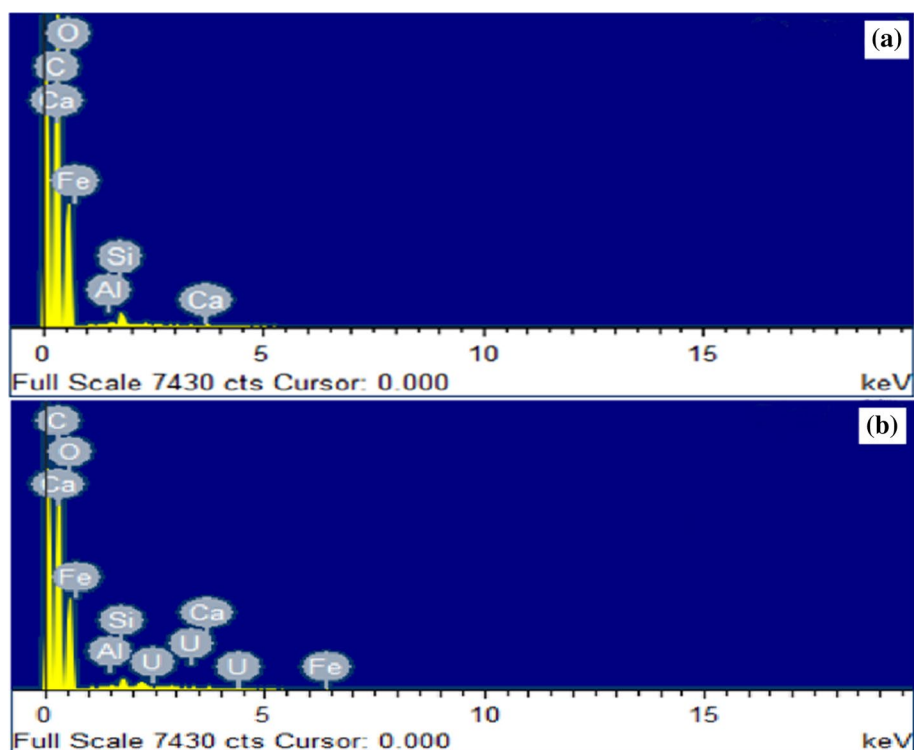**Fig. 3** EDS of **a** control biomass **b** uranium(VI) exposed biomass

Table 1 Elemental composition of control and uranium(VI) exposed biomass (obtained from EDS)

Elements	Biomass before adsorption of Uranium(VI)		Biomass after adsorption of Uranium(VI)	
	Weight %	Atomic %	Weight %	Atomic %
C	58.1	65.07	56.42	63.73
O	41.16	34.61	42.19	35.78
Al	0.09	0.04	0.14	0.07
Si	0.51	0.24	0.57	0.28
Ca	0.05	0.02	0.17	0.06
Fe	0.09	0.02	0.28	0.07
U	–	–	0.23	0.01
Total	100	100	100	100

Results and discussion

Effect of pH on the adsorption

To determine the optimum pH range for adsorptive action of the biomass batch experiments were carried out at different pH (1–13). The percentage removal of uranium(VI) as a function of pH is shown in Fig. 4. Initially, percentage removal was found to increase with the pH of the solution until pH 7, after that, percentage removal gradually decreased, indicating good agreement with similar studies [47, 48]. The maximum percentage removal of 97% was obtained at pH 7. With the increase in pH of the solution, the abundance of H^+ ions decreases, and hence the number of uranyl ions to be adsorbed on the surface increases [49]. At the same time, with increasing pH till 7, the tendency of uranyl ions to form hydrolyzed ions increases, which should get better adsorbed on the adsorbent surface. However, after pH 7, the uranyl ions tend to precipitate rather than adsorbed [11], and hence the percentage removal decreases after pH 7. Therefore, the optimum pH for adsorption by Vanda plant biomass is 7, which can be applied to remove uranium(VI) from potable water. Hence, this is a positive aspect of the uranium removal method. It is thus better than many reported methods for removal of uranium in which acidic pH was desired [46, 50–55].

Effect of contact time

To examine the contact time effects, about 0.1 g of biomass was added to 100 mL of 100 $\mu g\ L^{-1}$ uranium(VI) solution at pH 7, at 30 ± 5 °C temperature and the contact time was varied from 1 to 120 min. The observed effects of contact time are shown in Fig. 5. It was found that the percentage removal increases with the increasing contact time, and the equilibrium is achieved within 15 min after the contact. The uptake of uranium(VI) remains almost constant after 15 min, suggesting a fast adsorption process by the biomass. Adsorption of uranium(VI) by using this biomass is quick as compared to other adsorbents [48, 56, 57].

Fig. 4 Effect of pH on % removal, $C_i(U) = 100$ µg L^{-1}, contact time = 15 min, $T = 30 \pm 5$ °C, adsorbent dose = 0.1 g, volume = 100 mL
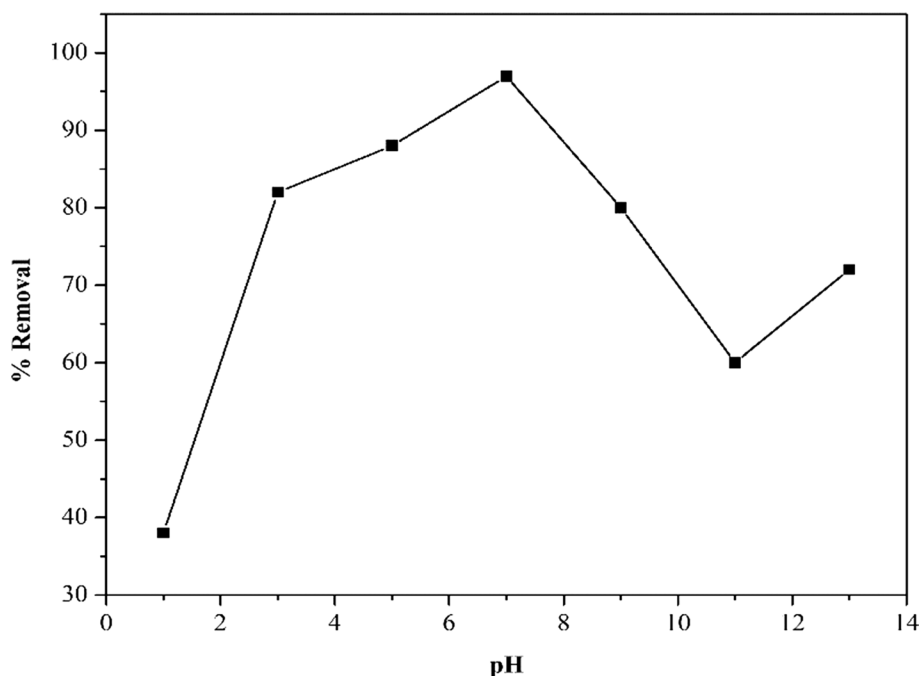
Fig. 5 Effect of contact time on % removal pH = 7, $T = 30 \pm 5$ °C, $C_i(U) = 100$ µg L^{-1}, adsorbent dose = 0.1 g, volume = 100 mL
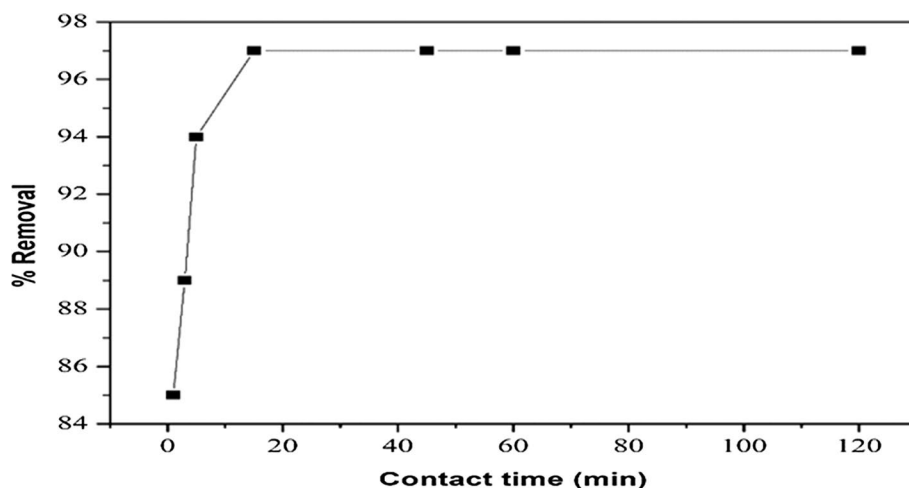
Effect of temperature

To understand the effect of temperature on uranium(VI) adsorption the experiments were carried out at 283 K, 293 K, 303 K, 313 K, 323 K, and 333 K temperatures. The graph prepared from the experimental data is shown in Fig. 6. This shows that percentage removal increases with temperature and it becomes constant after 303 K, or nearly at about room temperature.

Effect of adsorbent dosage

The effect of adsorbent dose (0.01 to 0.3 g) on the removal of uranium was studied under standard conditions (pH-7, contact time of 15 min, initial uranium concentration $C_i(U)$

as 100 µg L^{-1} present in 100 mL volume, and temperature between 30 ± 5 °C). The results obtained are presented in Fig. 7. This figure shows that percentage removal of uranium increases with increase in adsorbent dose till 0.1 g, which can be due to an increase in the number of active sites at the surface of the adsorbent. The adsorption efficiency shown in the secondary axis in Fig. 7 indicates that highest uptake capacity was obtained at a minimal dose of 0.01 g of biomass. Which projects adsorbent-solution ratio of 1:10 (mg: mL) is appropriate under the set of the test condition.

Maximum percentage removal was obtained at 0.1 g of biomass. On increasing the adsorbent dose after 0.1 g, the percentage removal remains constant.

Fig. 6 Effect of temperature on % removal, $C_i(U) = 100\ \mu g\ L^{-1}$, pH = 7, contact time = 15 min, adsorbent dose = 0.1 g, volume = 100 mL
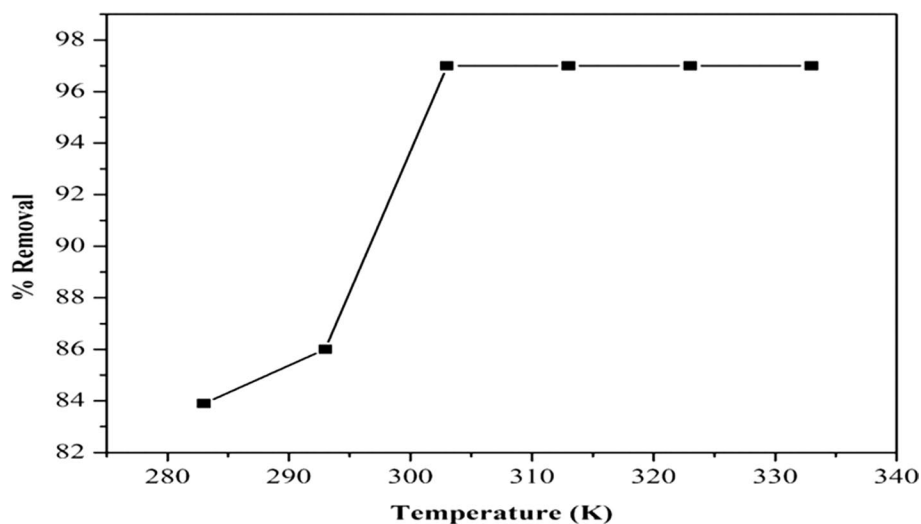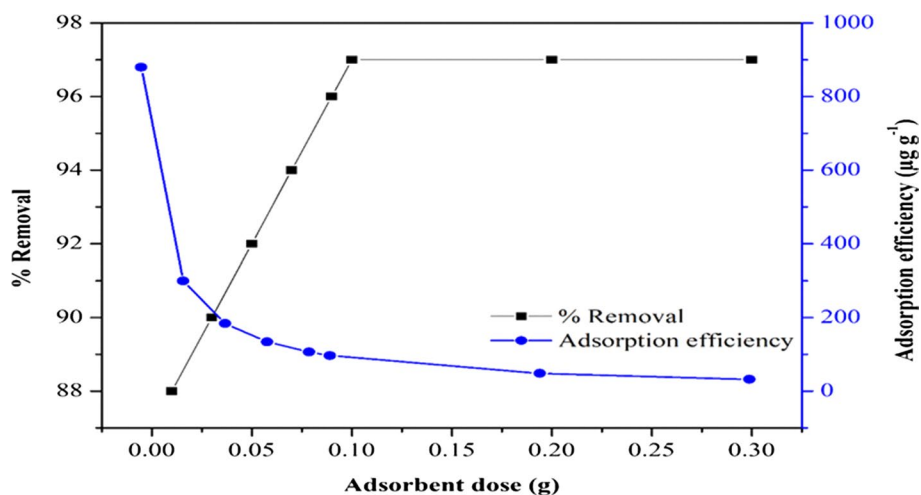

Fig. 7 Effect of adsorbent dose on % removal and adsorption efficiency $C_i(U) = 100\ \mu g\ L^{-1}$, pH = 7, contact time = 15 min, $T = 30 \pm 5$ °C, volume = 100 mL

Effect of initial ion concentration

The effect of initial ion concentration was elucidated by performing batch experiments at different initial ion concentrations (10–500 $\mu g\ L^{-1}$). Experimental data obtained is shown in Fig. 8, which shows that the percentage removal increases with an increase in initial ion concentration till 100 $\mu g\ L^{-1}$. After this the increase in adsorbate concentration decreases the adsorption efficiency. This behavior appears to be due to the saturation of active sites of the adsorbent. On the other hand, secondary axis data of Fig. 8 indicates that the uptake capacity of adsorbent increases with an increase in initial ion concentration; it is because with increasing initial ion concentration the driving force increases, which overcomes the mass transfer resistance between solid and liquid phases.

Effect of volume

To study the effect of volume on percentage removal, 0.1 g of biomass was added to different volumes of 100 $\mu g\ L^{-1}$ uranium solution (100 mL to 1000 mL). The volume dependence of percentage removal is shown in Fig. 9. The results show that percentage removal decreases with the increase in volume. The graph plotted between volume and uptake capacity of biosorbent shown in Fig. 9, indicates that the uptake capacity of adsorbent increases with an increase in volume. Hence, biosorbent can perform efficiently, even on a large adsorbate volume.

Fig. 8 Effect of initial concentration on % removal and adsorption efficiency, pH = 7, contact time = 15 min, volume = 100 mL, adsorbent dose = 0.1 g, $T = 30 \pm 5$ °C
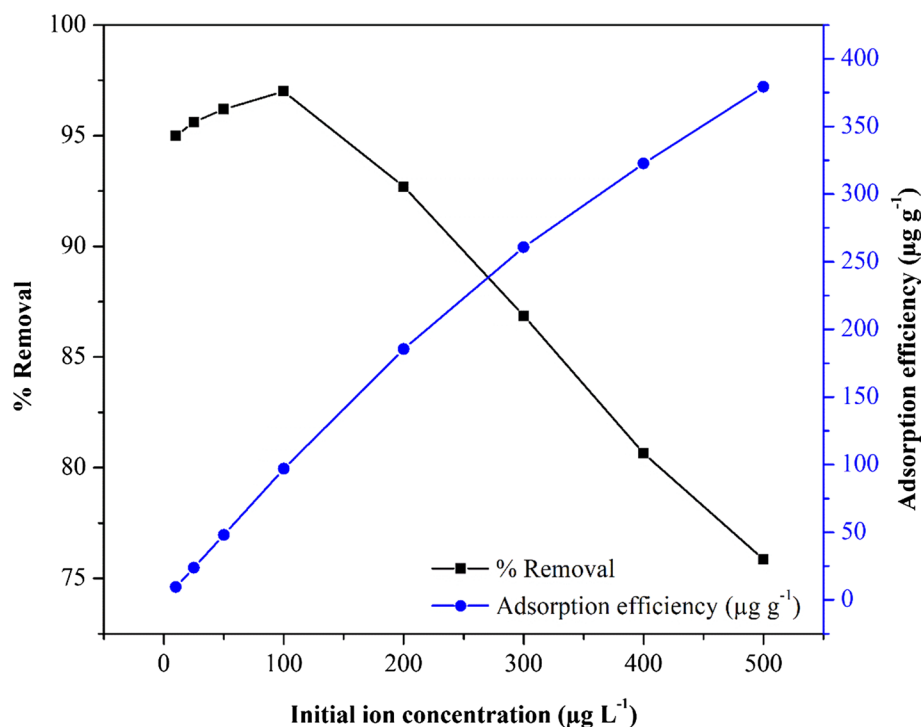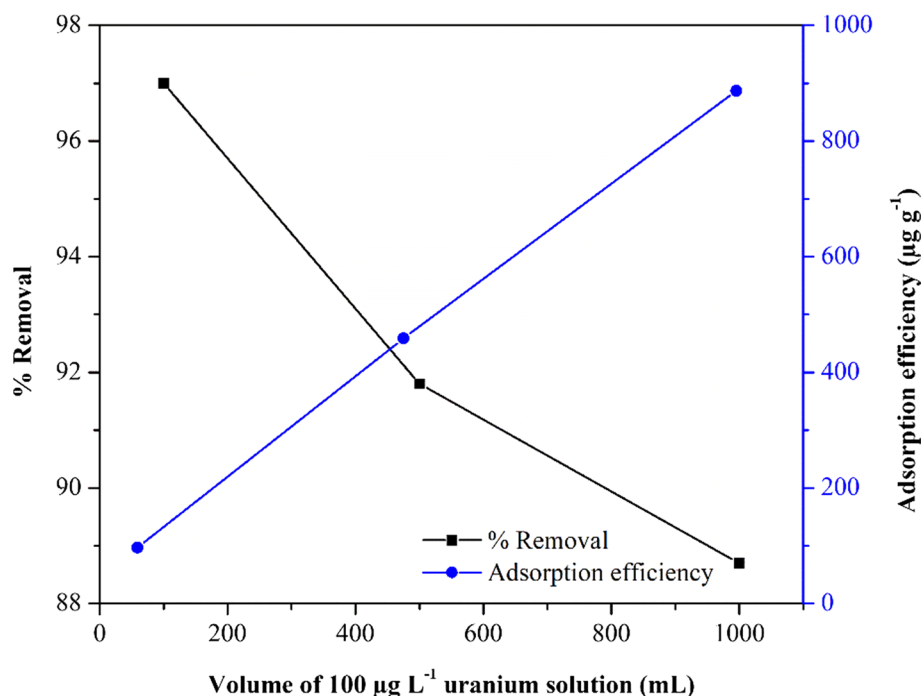
Fig. 9 Effect of volume on adsorption efficiency, pH = 7, contact time = 15 min, C_i (U) = 100 μg L^{-1}, adsorbent dose = 0.1 g, $T = 30 \pm 5$ °C

Adsorption isotherm study

Langmuir and Freundlich adsorption isotherm models were applied to evaluate the experimental data. Langmuir isotherm linear equation is shown in Eq. (4)

$$C_e/q_e = 1/bQ_0 + C_e/Q_0 \tag{4}$$

where q_e is the amount of metal ion adsorbed by biosorbent (μg g^{-1}), C_e is equilibrium concentration in solution (μg L^{-1}), Q_0 is maximum adsorption capacity (μg g^{-1}), and b is Langmuir constant (L μg^{-1}). A plot of C_e versus C_e/q_e
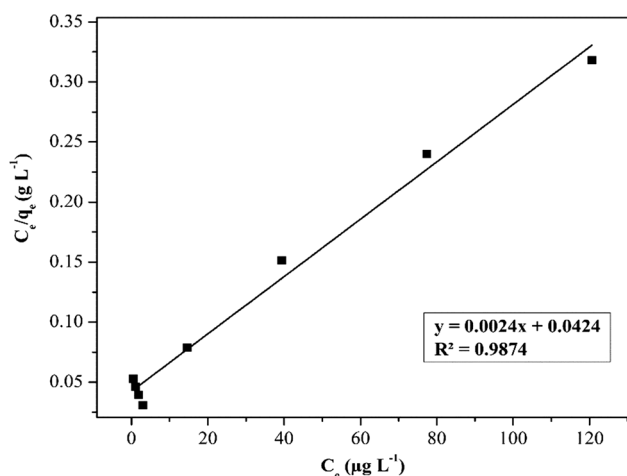
Fig. 10 Langmuir isotherm for uranium(VI) adsorption onto Vanda plant biomass, pH=7, time=15 min, $T=30\pm5$ °C, volume=100 mL, adsorbent dose=0.1 g

Table 2 Langmuir and Freundlich constants

Langmuir model			Freuidlich model		
R^2	Q_0 (µg g^{-1})	b (L µg^{-1})	R^2	K_F (µg g^{-1})	n
0.987	416.6	0.057	0.919	26.01	1.6

(shown in Fig. 10) yields a straight line with a correlation coefficient of 0.987. It suggests that experimental data is indicating good agreement with the Langmuir isotherm model. The Q_0 and b were calculated by the slope and intercept of the graph (shown in Table 2). Maximum adsorption efficiency (Q_0) of 416 µg g^{-1} was obtained by Langmuir adsorption isotherm.

Separation factor or equilibrium parameter, R_L: the fundamental characteristic of Langmuir

isotherm was calculated by the Eq. (5)

$$R_L = 1/\left(1 + bC_i\right) \tag{5}$$

where b is the Langmuir constant (L µg^{-1}), and C_i is the initial ion concentration (µg L^{-1}). R_L values were found $0 < R_L < 1$, which indicates the adsorption of uranium(VI) on to Vanda biomass is favorable. R_L value decreases with increasing concentration (shown in Fig. 11). The lower value of R_L for higher-level indicates that adsorption is more advantageous in higher concentrated uranium solution taken in this study [50].

Freundlich isotherm linear equation is shown in Eq. (6)

$$\ln q_e = \ln K_F + 1/n \ln C_e \tag{6}$$

n and K_F are constants, calculated from the slope and intercept of the graph plotted between $\ln C_e$ and $\ln q_e$. Calculated
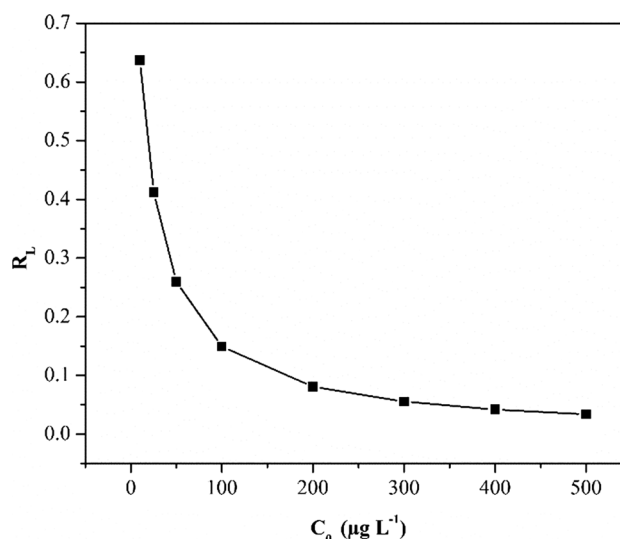

Fig. 11 Graph plotted between R_L and initial ion concentration (C$_0$), pH=7, time=15 min, $T=30\pm5$ °C, volume=100 mL, adsorbent dose=0.1 g

values are given in Table 2. R^2 value (0.987) indicates that experimental data is showing good agreement with the Langmuir isotherm model. While experimental data is also having satisfactory agreement with the Freundlich isotherm model, R^2 (0.919) but the value of K_F obtained from Freundlich isotherm model is not showing consistency with experimental data (given in Table 3) meanwhile the adsorption efficiency obtained from Langmuir isotherm model shows perfect agreement with experimentally obtained data.

Thermodynamic study

Thermodynamic parameters: Gibbs free energy (ΔG^0), enthalpy (ΔH^0), and entropy (ΔS^0) have been calculated by the Eqs. (7), (8), and (9) and given in Table 4.

$$\Delta G^0 = \Delta H^0 - T\Delta S^0 \tag{7}$$

$$\Delta G^0 = -RT \ln K \tag{8}$$

$$-\ln K = \Delta H^0/RT - \Delta S^0/R \tag{9}$$

where K is the distribution coefficient, ΔH^0 is standard enthalpy (kJ mol^{-1}), ΔS^0 is standard entropy (J mol^{-1} K^{-1}), T is the absolute temperature (K), R is the gas constant (8.314 J mol^{-1} K^{-1}), and ΔG^0 (kJ mol^{-1}) is standard Gibbs free energy.

Values of enthalpy change (ΔH^0) and entropy change (ΔS^0) were calculated by the slope and intercept of the graph plotted between $1/T$ and $\ln K$ (shown in Fig. 12).

Table 3 Experimentally obtained adsorption efficiency

Experimentally obtained data								
Initial concentration C_0 (µg L^{-1})	10	25	50	100	200	300	400	500
Adsorption efficiency q_e (µg g^{-1})	9.5	23.9	48.1	97	185.4	260.6	322.6	379.3

Table 4 Thermodynamic parameters for uranium removal on to Vanda biomass

ΔH^0 (kJ mol^{-1})	ΔS^0 (J mol^{-1} K^{-1})	ΔG^0 (kJ mol^{-1})			
		283 K	293 K	303 K	313 K
41.4	178.49	− 9.06	− 10.85	− 12.63	− 14.42

The positive value of ΔH^0 indicates the endothermic nature of adsorption, and positive values of ΔS^0 suggests an increase in randomness in the surface during adsorption processes. The halving of positive values of ΔH^0 and ΔS^0 indicates that the adsorption reaction is product favorable after a specific temperature. The graph plotted between temperature and percentage removal shows the maximum percentage removal at 303 K and then remains constant. The adsorption reaction is favored as ΔG^0 decreases with the increase in temperature [52]. Also, the negative value of ΔG^0 shows the spontaneous nature of adsorption.

Kinetics of adsorption

To assess the kinetics of uranium(VI) adsorption onto the Vanda plant biomass adsorbent, experimental data was applied with a pseudo-first-order kinetic model and pseudo-second-order kinetic model.

Linear expression of the pseudo-first-order model and second-order model can be given as Eq. (10) and (11), respectively

$$\text{Pseudo-first-order equation}: \ln\left(q_e - q_t\right) = \ln q_e - k_1 t \quad (10)$$

$$\text{Pseudosecond-order equation}: t/q_t = 1/k_2 q_e^2 + t/q_e \quad (11)$$

where q_t and q_e are the amount of uranium(VI) ion adsorbed (µg g^{-1}) at time t (min) and at equilibrium time, respectively, k_1 (min^{-1}) and k_2 (g µg^{-1} min^{-1}) are pseudo-first-order and second-order sorption constants respectively.

It can be interpreted from the graph plotted between t/q_t versus t, that the experimental data shows good agreement with the pseudo-second-order model with a correlation value of 1. Values of q_e (amount of uranium adsorbed at equilibrium time), k (rate constant for pseudo-first and second-order model) are given in Table 5.

Validation and application of the *Vanda tessellata* based biosorbent

The proposed method was applied to natural uranium contaminated ground water samples. Ground water samples were collected from Rajnandgaon district (Koudikasa village) of Chhattisgarh. Ground water sample no. 1 and 2 were
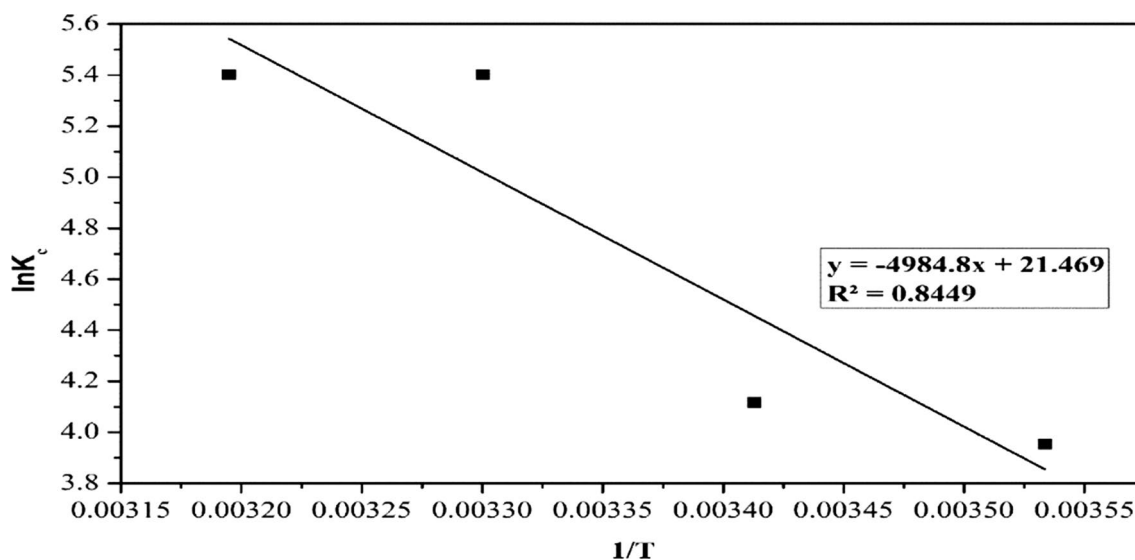

Fig. 12 Plot of ln K versus $1/T$ for uranium(VI) adsorption (pH = 7, adsorbent dose = 0.1 g, volume = 100 mL, initial uranium concentration = 100 µg L^{-1}, T = 30 ± 5 °C) by Vanda plant biomass

Table 5 Kinetic parameters for uranium adsorption on to Vanda biomass

	R^2	Rate constant (k)	q_e (calculated) ($\mu g\ g^{-1}$)	q_e (experimental) ($\mu g\ g^{-1}$)
Pseudo-first-order kinetic model	0.483	0.0015 (min^{-1})	1.077	97.00
Pseudo-second-order kinetic model	1	0.17 ($g\ \mu g^{-1}\ min^{-1}$)	97.087	

Table 6 Ground water sample analysis taken for validation of proposed method

Parameter	Groundwater sample 1	Groundwater sample 2
pH	6.9	7.1
TDS ($mg\ L^{-1}$)	627	417
EC ($\mu S\ cm^{-1}$)	1279	850
ORP (mV)	29.8	19.8
Fluoride ($mg\ L^{-1}$)	0.5	0.7
Chloride ($mg\ L^{-1}$)	151	72
Nitrate ($mg\ L^{-1}$)	38	36
Sulphate ($mg\ L^{-1}$)	54	36
Phosphate ($mg\ L^{-1}$)	BDL	BDL
Total hardness ($mg\ L^{-1}$)	440	310
Calcium hardness ($mg\ L^{-1}$)	310	215
Magnesium hardness ($mg\ L^{-1}$)	130	95
Total alkalinity ($mg\ L^{-1}$)	250	200
Carbonate ($mg\ L^{-1}$)	25	BDL
Bicarbonate ($mg\ L^{-1}$)	225	200
As ($mg\ L^{-1}$)	BDL	BDL
Pb ($mg\ L^{-1}$)	BDL	BDL
U ($\mu g\ L^{-1}$)	18.3	13.6
% Removal of uranium by *Vanda tessellata* biomass	95%	94.2%

BDL Below detection limit

collected from latitude 20.7251, longitude 80.72892 and latitude 20.67407, longitude 80.7718 respectively. Standard sampling and analysis protocols were adopted. The uranium concentration and associated water quality parameters of water samples were analyzed by the standard procedures [58] (results shown in Table 6).

To validate the results of *Vanda tessellata* based biosorbent lab study obtained as above, we conducted uranium adsorption experiments, in natural ground water samples found contaminated with naturally occurring uranium. The biomass was applied to the natural water samples in triplicate samples. Briefly, about 0.1 g of biomass was added to 100 mL of 100 μg L^{-1} uranium solution at pH 7, at $30 \pm 50C$ temperature and the contact time of 15 min. It was observed that in both samples removal of uranium was more than 94%. A good agreement between the data obtained with synthetic and the natural samples validate the proposed method for uranium removal from natural samples.

Conclusion

This study reports a systematic investigation on the adsorption properties of the orchid plant *Vanda tessellata*. Various adsorption properties, optimum ranges of various parameters, kinetics, thermodynamics, and mechanisms of adsorption are is reported. The orchid *Vanda tessellata* is identified as an efficient adsorbent for removing uranium from the aqueous medium at pH 7. The optimal removal can be reached in 15 min at a small dose of biomass. It was noted that the increasing concentration of uranium(VI) decreases the removal percentage. Experimental data showed good agreement with Langmuir adsorption isotherm ($R^2 = 0.987$). This indicates that the adsorption by *Vanda tessellata* biomass is predominantly a monolayered adsorption process. Using the Langmuir adsorption isotherm the maximum adsorption capacity was calculated as 416 μg uranium(VI) per gram of biomass. FTIR study indicates the involvement of N–H, O–H, C–O–C groups in the sorption of uranyl ions. The negative Gibbs free energy ($- 12.6$ kJ mol^{-1}) at optimum temperature 303 K and positive enthalpy; ($\Delta H = 41.4$ kJ mol^{-1}) indicate that the adsorption process is spontaneous and endothermic. The pseudo-second-order kinetic model showed a relatively high correlation coefficient ($R^2 = 1$) value, describing good applicability of the adsorption dynamics. Sucessful application of the studied biomass on some naturally uranium contaminated samples obtained from village Koudikasa in Chhattisgarh state, validates the efficacy of the biosorbent in treating natural samples also.

Compliance with ethical standards

References

1. Keith S, Faroon O, Roney N, Scinicariello F, Wiber S, Lngerman L, Llados F, Plewak D, Wohlers D, Diamond G (2013)

Toxicological profile for uranium. Agency for Toxic Substances and Disease Registry (US), Atlanta (GA)

2. Kale A, Bandela N, Kulkarni J (2020) Assessment of chemo-radiological risk of naturally occurred uranium in groundwater from the Beed district, India. J Radioanal Nucl Chem 323:151–157. https://doi.org/10.1007/s10967-019-06849-3

3. World Health Organization (2011) Guidelines for drinking water. World Health Organization, Geneva

4. AERB (Atomic Energy Regulatory Board) (2004) Directive for limit on uranium in drinking water, Mumbai, India

5. Yadav AK, Sahoo SK, Mahapatra S, Kumar AV, Pandey G, Lenka P, Tripathi RM (2014) Concentrations of uranium in drinking water and cumulative, age-dependent radiation doses in four districts of Uttar Pradesh, India. Toxicol Environ Chem 96:192–200. https://doi.org/10.1080/02772248.2014.934247

6. Tan Y, Le L, Zhang H, Ding D, Dai Z, Xue J, Liu J, Hu N, Wang Y (2018) Adsorption and recovery of U(VI) from actual acid radioactive wastewater with low uranium concentration using thioacetamide modified activated carbon from liquorice residue. J Radioanal Nucl Chem 317:811–824. https://doi.org/10.1007/s10967-018-5952-8

7. Ahmed SH, Sharaby CM, El Gammal EM (2013) Uranium extraction from sulfuric acid medium using trioctylamine impregnated activated carbon. Hydrometallurgy 134–135:150–157. https://doi.org/10.1016/j.hydromet.2013.02.003

8. Afsari M, Safdari J, Towfighi J, Mallah MH (2012) The adsorption characteristics of uranium hexafluoride onto activated carbon in vacuum conditions. Ann Nucl Energy 46:144–151. https://doi.org/10.1016/j.anucene.2012.03.031

9. Bayramoglu G, Arica MY (2016) MCM-41 silica particles grafted with polyacrylonitrile: modification in to amidoxime and carboxyl groups for enhanced uranium removal from aqueous medium. Microporous Mesoporous Mater 226:117–124. https://doi.org/10.1016/j.micromeso.2015.12.040

10. Abubakar M, Tamin MN, Saleh MA, Uday MB, Ahmad N (2016) Preparation and characterization of a nigerian mesoporous clay-based membrane for uranium removal from underground water. Ceram Int 42:8212–8220. https://doi.org/10.1016/j.ceramint.2016.02.031

11. Nekhunguni PM, Tavengwa NT, Tutu H (2017) Sorption of uranium(VI) onto hydrous ferric oxide-modified zeolite: Assessment of the effect of pH, contact time, temperature, selected cations and anions on sorbent interactions. J Environ Manag 204:571–582. https://doi.org/10.1016/j.jenvman.2017.09.034

12. Shao L, Wang X, Ren Y, Wang S, Zhong J, Chu M, Tang H, Lue L, Xie D (2016) Facile fabrication of magnetic cucurbit[6]uril/graphene oxide composite and application for uranium removal. Chem Eng J 286:311–319. https://doi.org/10.1016/j.cej.2015.10.062

13. Mahfouz MG, Galhoum AA, Gomaa NA, Abdel-rahem SS, Atiya AA, Vincent T, Guibal E (2015) Uranium extraction using magnetic nano-based particles of diethylenetriamine-functionalized chitosan: equilibrium and kinetic studies. Chem Eng J 262:198–209. https://doi.org/10.1016/j.cej.2014.09.061

14. Wei J, Zhang X, Liu Q, Li Z, Liu L, Wang J (2014) Magnetic separation of uranium by $CoFe_2O_4$ hollow spheres. Chem Eng J 241:228–234. https://doi.org/10.1016/j.cej.2013.12.035

15. Kryvoruchko AP, Yurlova LY, Atamanenko ID, Korinilovich BY (2004) Ultrafiltration removal of U(VI) from contaminated water. Desalination 162:229–236. https://doi.org/10.1016/S0011-9164(04)00046-3

16. Zhang L, Zhang X, Lu Q, Wu X, Jiang T, Mi L, Peng Y (2019) Adsorption of U(VI) ions from aqueous solution using nanogoethite powder. Adsorpt Sci Technol 37:113–126. https://doi.org/10.1177/0263617418816202

17. Nilchi A, Shariati Dehaghan T, Rasouli Garmarodi S (2013) Kinetics, isotherm and thermodynamics for uranium and thorium ions adsorption from aqueous solutions by crystalline tin oxide nanoparticles. Desalination 321:67–71. https://doi.org/10.1016/j.desal.2012.06.022

18. Sadeghi S, Azhdari H, Arabi H, Moghaddam AZ (2012) Surface modified magnetic Fe_3O_4 nanoparticles as a selective sorbent for solid phase extraction of uranyl ions from water samples. J Hazard Mater 215–216:208–216. https://doi.org/10.1016/j.jhazmat.2012.02.054

19. Kong L, Zhu Y, Wang M, Li Z, Tan Z, Xu R, Tang H, Chang X, Xiong Y, Chen D (2016) Simultaneous reduction and adsorption for immobilization of uranium from aqueous solution by nano-flake Fe-SC. J Hazard Mater 320:435–441. https://doi.org/10.1016/j.jhazmat.2016.08.060

20. Wang Y, Gu Z, Yang J, Liao J, Yang Y, Liu N, Tang J (2014) Amidoxime-grafted multiwalled carbon nanotubes by plasma techniques for efficient removal of uranium(VI). Appl Surf Sci 320:10–20. https://doi.org/10.1016/j.apsusc.2014.08.182

21. Kar AS, Kumar S, Tomar BS (2012) U(VI) sorption by silica: effect of complexing anions. Colloids Surf Physicochem Eng Asp 395:240–247. https://doi.org/10.1016/j.colsurfa.2011.12.038

22. Gao J-K, Hou L-A, Zhang G-H, Gu P (2015) Facile functionalized of SBA-15 via a biomimetic coating and its application in efficient removal of uranium ions from aqueous solution. J Hazard Mater 286:325–333. https://doi.org/10.1016/j.jhazmat.2014.12.061

23. Vivero-Escoto JL, Carboni M, Abney CW, DeKrafft KE, Lin W (2013) Organo-functionalized mesoporous silicas for efficient uranium extraction. Microporous Mesoporous Mater 180:22–31. https://doi.org/10.1016/j.micromeso.2013.05.030

24. Ivanova B, Spiteller M (2014) Adsorption of uranium composites onto saltrock oxides—experimental and theoretical study. J Environ Radioact 135:75–83. https://doi.org/10.1016/j.jenvrad.2014.03.019

25. Khani MH, Keshtkar AR, Ghannadi M, Pahlavanzadeh H (2008) Equilibrium, kinetic and thermodynamic study of the biosorption of uranium onto *Cystoseria indica* algae. J Hazard Mater 150:612–618. https://doi.org/10.1016/j.jhazmat.2007.05.010

26. Bajwa BS, Kumar S, Singh S, Sahoo SK, Tripathi RM (2017) Uranium and other heavy toxic elements distribution in the drinking water samples of SW-Punjab, India. J Radiat Res Appl Sci 10:13–19. https://doi.org/10.1016/j.jrras.2015.01.002

27. Saini K, Bajwa BS (2016) Uranium distribution study in the drinking water samples of SW Punjab, India. Adv Appl Sci Res 7(2):103–108

28. Narang S, Kumar D, Kumar A (2018) Health-related analysis of uranium in Fazilka district, Punjab, India. Curr Sci 115:2079

29. Nagaiah N, Mathews G, Balakrishna KK, Ranjana AM, Naregundi K (2013) Influence of physico-chemical parameters on the distribution of uranium in the ground water of Bangalore, India. Radiat Prot Environ 36:175–180

30. Rani A, Mehra R, Duggal V, Balaram V (2013) Analysis of uranium concentration in drinking water samples using ICPMS. Health Phys 104:251–255. https://doi.org/10.1097/HP.0b013e318279ba05

31. Gascoyne M (1989) High levels of uranium and radium in groundwaters at Canada's Underground Research Laboratory, Lac du Bonnet, Manitoba, Canada. Appl Geochem 4:577–591. https://doi.org/10.1016/0883-2927(89)90068-1

32. Amakom C, Jibiri N (2010) Chemical and radiological risk assessment of uranium in borehole and well waters in the Odeda Area, Ogun State, Nigeria. Int J Phys Sci 5:1009–1014

33. Stalder E, Blanc A, Haldimann M, Dudler V (2012) Occurrence of uranium in Swiss drinking water. Chemosphere 86:672–679. https://doi.org/10.1016/j.chemosphere.2011.11.022

34. Vesterbacka P, Mäkeläinen I, Arvela H (2005) Natural radioactivity in drinking water in private wells in Finland. Radiat Prot Dosim 113:223–232. https://doi.org/10.1093/rpd/nch446

35. Prakash B, Bais RT (2016) A Novel chemical compound from the leaf extract of Vanda tessellata (Roxb.) Hook. ex G. Don. World J Pharm Res 5:10

36. Ricks AM, Gagliardi L, Duncan MA (2010) Infrared spectroscopy of extreme coordination: the carbonyls of U^+ and UO_2^+. J Am Chem Soc 132:15905–15907. https://doi.org/10.1021/ja1077365

37. Sahu C, Khan F, Pandey PK, Pandey M (2017) Biosorptive removal of toxic contaminant lead from wastewater. Asian J Chem 29:650–656

38. Sahu C, Khan F, Pandey PK, Pandey M (2017) Proficient removal of As (III) from water using orchid plant (Vanda sp.) as biosorbent. Asian J Chem 29:1790–1796

39. Gardiner LM, Kocyan A, Motes M, Robert DL, Emerson BC (2013) Molecular phylogenetics of *Vanda* and related genera (Orchidaceae): Molecular Phylogenetics of *Vanda*. Bot J Linn Soc 173:549–572. https://doi.org/10.1111/boj.12102

40. Sahu SK, Maity S, Bhangare RC, Pandit GG, Sharma DN (2014) Determination of uranium in ground water using different analytical technique, vol 34. Bhabha Atomic Research Centre, Mumbai

41. Tian G, Geng J, Jin Y, Wang C, Li S, Chen Z, Wang H, Zhao Y, Li S (2011) Sorption of uranium(VI) using oxime-grafted ordered mesoporous carbon CMK-5. J Hazard Mater 190:442–450. https://doi.org/10.1016/j.jhazmat.2011.03.066

42. Coates J (2006) Interpretation of infrared spectra, a practical approach. Encycl Anal Chem Appl Theory Instrum 1–23

43. Wang J, Zhuang S (2019) Extraction and adsorption of U(VI) from aqueous solution using affinity ligand-based technologies: an overview. Rev Environ Sci Biotechnol 18(3):437–452

44. Wang X, Xia L, Tan K, Zheng W (2012) Studies on adsorption of uranium (VI) from aqueous solution by wheat straw. Environ Prog Sustain Energy 31:566–576

45. Yusan SD, Erenturk SA (2011) Sorption behaviors of uranium (VI) ions on α-FeOOH. Desalination 269:58–66

46. Xiao-teng Z, Dong-mei J, Yi-qun X, Jun-chang C, Shuai H, Liang-shu X (2019) Adsorption of uranium(VI) from aqueous solution by modified rice stem. J Chem 2019:1–10. https://doi.org/10.1155/2019/6409504

47. Yu J, Wang J, Jiang Y (2017) Removal of uranium from aqueous solution by alginate beads. Nucl Eng Technol 49:534–540. https://doi.org/10.1016/j.net.2016.09.004

48. Rong L, Zeming S, Yun H, Kailiang Z, Junji Z, Xinyu W, Ke C, Lvhang Y (2019) Uranium sorption onto mullite: characteristics of isotherms, kinetics and thermodynamics. J Earth Syst Sci 128:176

49. Saha R, Das S, Banerjee A, Sahana A, Sudarsan M, Slawin AMZ, Li Y, Das D (2010) pH dependent separation of uranium by chelation chromatography using pyridine 2,6-dimethanol as a chelator: single crystal X-ray structural confirmation of the chelated uranium complex. J Hazard Mater 181:154–160. https://doi.org/10.1016/j.jhazmat.2010.04.111

50. Zhao Y, Liu C, Feng M, Chen Z, Li S, Tian G, Wang L, Huang J, Li S (2010) Solid phase extraction of uranium(VI) onto benzoylthiourea-anchored activated carbon. J Hazard Mater 176:119–124. https://doi.org/10.1016/j.jhazmat.2009.11.005

51. Hazer O, Kartal Ş (2010) Use of amidoximated hydrogel for removal and recovery of U(VI) ion from water samples. Talanta 82:1974–1979. https://doi.org/10.1016/j.talanta.2010.08.023

52. Aytas S, Turkozu DA, Gok C (2011) Biosorption of uranium(VI) by bi-functionalized low cost biocomposite adsorbent. Desalination 280:354–362. https://doi.org/10.1016/j.desal.2011.07.023

53. Sert Ş, Eral M (2010) Uranium adsorption studies on aminopropyl modified mesoporous sorbent (NH2–MCM-41) using statistical design method. J Nucl Mater 406:285–292. https://doi.org/10.1016/j.jnucmat.2010.08.024

54. Song Q, Ma L, Liu J, Bai C, Geng J, Wang H, Li B, Wang L, Li S (2012) Preparation and adsorption performance of 5-azacytosine-functionalized hydrothermal carbon for selective solid-phase extraction of uranium. J Colloid Interface Sci 386:291–299. https://doi.org/10.1016/j.jcis.2012.07.070

55. Yusan S, Akyil S (2008) Sorption of uranium(VI) from aqueous solutions by akaganeite. J Hazard Mater 160:388–395. https://doi.org/10.1016/j.jhazmat.2008.03.009

56. Kushwaha S, Sudhakar PP (2013) Sorption of uranium from aqueous solutions using palm-shell-based adsorbents: a kinetic and equilibrium study. J Environ Radioact 126:115–124

57. Wang G, Wang X, Chai X, Liu J, Deng N (2010) Adsorption of uranium (VI) from aqueous solution on calcined and acid-activated kaolin. Appl Clay Sci 47:448–451. https://doi.org/10.1016/j.clay.2009.11.003

58. APHA (1999) Standard methods for the examination of water and wastewater. In: Water environment federation american water works association, 23rd edition. American Public Health Association, Washington, DC